Berkala **PENELITIAN HAYATI**

ISSN: 08526834 | E-ISSN:2337-389X

Volume 31 | No. 3 | **December** | 2025

Original article

Spatial Identification of Carbon Stock Hotspots for Urban Climate Mitigation Planning: Remote Sensing Analysis of Malang City, Indonesia

Dina Resmeitasari[1]*, Bambang Semedi[2], Wresti L. Anggayasti[3]

[1] Environmental and Development Resources Management Master's Study Program, Graduate School of Brawijaya University, Jl. Veteran Kota Malang 65141, Indonesia

[2] Faculty of Fisheries and Marine Sciences of Brawijaya University, Jl. Veteran Kota Malang 65141, Indonesia

[3] Graduate School of Brawijaya University, Jl. Veteran Kota Malang 65141, Indonesia

Abstract

Urban expansion in tropical cities threatens carbon storage through vegetation-to-built conversion. Malang City, Indonesia, experiences accelerating vegetation loss due to urban sprawl. Here, spatially detailed assessments linking vegetation conversion to carbon dynamics remain absent, limiting evidence-based climate governance. This study thus employs high-resolution remote sensing integrated with spatial analysis to quantify carbon stock dynamics and identify priority intervention zones in a rapidly urbanizing tropical city context. Understanding carbon loss magnitude and geographic concentration is essential for targeted interventions. Google Dynamic World satellite data were processed through Google Earth Engine and validated against ground truth. Carbon stocks were estimated with international standard and reclassified according to national greenhouse gas mitigation guidelines. Linear regression characterized temporal trends; spatial analysis identified carbon release hotspots and sequestration opportunity areas. Results show that Malang City experienced an average annual carbon stock decline of 6,803.80 tC per year between 2016 and 2025, representing a considerable overall loss. Carbon release hotspots concentrated in southern and southeastern urban-fringe zones due to vegetation-to-built conversion, while sequestration areas remained in fragmented northern and eastern patches. Hotspot permanence classification identified areas requiring urgent protection and areas retaining restoration potential. Spatially-explicit hotspot identification provides municipalities with an actionable framework for climate-responsive planning and targeted mitigation. This study demonstrates method applicability to other tropical cities seeking evidence-based urban carbon policy.

Keywords: carbon dynamics, carbon hotspots, carbon stock, Google Dynamic World, land cover change, urban climate mitigation

Received: November 13, 2025 | Revised: December 15, 2025 Accepted: December 25, 2025

Introduction

Climate change has emerged as a global complex issue driven by increased greenhouse gas (GHG) concentrations in the atmosphere, including CO_2. In particular, The Agriculture, Forestry, and Other Land Use (AFOLU) sector contributes significantly to CO_2 emissions through conversion of natural ecosystems, which releases stored carbon reserves. Therefore, understanding Land Cover Change (LCC) dynamics constitutes a critical key to climate change mitigation efforts at national and regional levels (IPCC, 2019).

The LCC dynamics in urban regions of Indonesia are driven by accelerated population growth, spatial demand for residential settlements, infrastructure, and public facilities, resulting in increased built-up area expansion and deteriorating environmental quality (Pambudi et al., 2024). In line with the condition of Indonesia, Malang City, as the second-largest city in East Java Province, exemplifies this challenge, experiencing significant built-up area expansion and declining vegetation coverage (Isdianto et al., 2025). Projections of greenhouse gas emissions from Malang City's transportation sector are estimated to reach 6 million tons CO_2-eq by 2034 (Nandini et al., 2024), affirming the urgency of measured carbon mitigation interventions based on spatial data.

Managing the complexity and rapid pace of LCC dynamics in urban regions requires highly accurate spatial data with high temporal resolution. Remote sensing has emerged as an effective environmental monitoring tool (Semedi et al., 2021). The Dynamic World (DW) platform, operating on Google Earth Engine, offers an innovative solution by providing global land cover maps at 10-meter spatial resolution with near real-time daily updates, far exceeding conventional land cover data in temporal resolution (Venter et al., 2022). DW classifies land cover into nine probability classes, enabling researchers to track rapid changes with high accuracy. Spatially and temporally rich DW data represents crucial input for carbon stock estimation models, particularly for correlating land conversion rates with carbon emission factors. Conversion to built-up areas reduces ecosystem capacity for carbon storage, so LCC in urban areas tends to reduce carbon stock values (Rahman et al., 2023) and threatens urban environmental carrying capacity.

Prior research demonstrates the utility of remote sensing for urban carbon stock mapping. Tavasoli et al. (2019) utilized ALOS PALSAR and Sentinel data to model urban forest carbon stocks with R^2 accuracy of 0.60–0.83. Liu et al. (2025) employed hotspot analysis

* Corresponding Author:
Dina Resmeitasari
Environmental and Development Resources Management Master's Study Program, Graduate School of Brawijaya University, Jl. Veteran Kota Malang 65141, Indonesia
Phone: +6281805080291
E-mail: resmeitasaridina@gmail.com

(Getis-Ord Gi*) to identify spatial clustering patterns of carbon sequestration capacity. However, these studies suffered from limited temporal resolution without specific identification of degradation hotspots. Cahyono et al. (2022) analyzed CO_2 emissions and sequestration across 32 Indonesian cities; yet spatially explicit analyses remain rarely applied in Indonesian urban contexts where rapid urban sprawl creates heterogeneous carbon loss and retention patterns.

This research thus aims to address these gaps through several methodological innovations: (1) utilizing DW data to track Malang City's LCC dynamics from 2016 to 2025; (2) conducting comprehensive spatial analysis to identify and map specific locations experiencing carbon degradation and areas with high sequestration capacity, to provide priority guidance for mitigation, conservation, and restoration strategies; (3) integrating IPCC Tier 1 method with high-resolution remote sensing and real-time temporal dynamics; (4) identifying entrenched degradation hotspots to support development of a Climate-Centric Zoning framework; and (5) enabling continuous monitoring for adaptive management. Through these mechanisms, this research contributes to advance understanding of urban carbon dynamics and provides empirical evidence and methodological framework for local-level climate change mitigation efforts in rapidly urbanizing tropical regions.

Methods

This research employs a quantitative spatial approach utilizing remote sensing technology and Geographic Information Systems (GIS). The study location focuses on the administrative region of Malang City, East Java Province, covering 11,108 hectares, situated at 7°54'39"–8°3'5" South Latitude, 112°34'8"–112°41'37" East Longitude. The research framework involves four primary stages: (1) acquisition and pre-processing of temporal land cover data; (2) classification and validation of temporal land cover data; (3) carbon stock inventory and quantification; (4) carbon stock change and temporal dynamics analysis; and (5) spatial analysis of carbon release and carbon sequestration. This research is descriptive-analytical in nature, quantifying the rate of carbon stock change caused by LCC in Malang City during the 2016–2025 period.

Acquisition and Pre-Processing of Temporal Land Cover Data

Primary spatial land cover data were obtained from the Dynamic World (DW) platform, accessed through Google Earth Engine (GEE). DW data are supplied in raster map format with 9 land cover classes (water, trees, grass, flooded vegetation, crops, shrub and scrub, built, bare, and snow and ice) at 10-meter spatial resolution. The selection of DW is based on its advantages in providing land cover data with high spatial resolution (10 meters) and daily (near real-time) temporal resolution, derived from Sentinel-2 satellite imagery (Brown et al., 2022). DW data were compiled to generate classified land cover maps for the initial period (2016) and final period (2025), encompassing nine land cover classes.

Pre-processing ensured spatial-temporal consistency through systematic stages. First, annual DW image composites (January–December) were selected to reduce seasonal variability and cloud interference effects, providing more robust permanent land cover conditions than single-date imagery. Second, coordinate system transformation was applied from local projections to EPSG:4326 (WGS84) for Google Earth Engine compatibility. Third, boundary geometry (area of interest) was defined from Malang City administrative shapefiles. Spatial and temporal filtering were applied to DW image collections using AOI boundary and observation year parameters. Annual composites were generated by applying mode statistical functions to obtain the dominant land cover class per pixel. Final processing involved clipping and converting results to align with original DW classification scheme. The entire procedure was executed using Google Earth Engine API integrated with QGIS, enabling efficient standardized processing of high-resolution data without requiring substantial local computing resources.

Classification and Validation of Temporal Land Cover Data

Land cover classification accuracy validation was conducted using the confusion matrix method to assess agreement between DW classification and field reference data (ground truth). Ground truth data were collected through field survey and visual interpretation of very high-resolution (VHR) satellite imagery from Google Earth imagery for 2025. A total of 100 stratified random sampling points were distributed across each land cover class.

From the confusion matrix, several accuracy metrics were calculated: (1) Overall Accuracy (OA), representing the proportion of correctly classified total pixels; (2) Producer's Accuracy (PA), measuring omission error or failure to detect a specific class; (3) User's Accuracy (UA), measuring commission error or incorrect pixel assignment to a class; and (4) Kappa Coefficient (κ), measuring agreement between classification and reference while accounting for chance agreement (NV5 Geospatial Solutions, 2024).

The Kappa coefficient was calculated using the formula:

$$\kappa = \frac{N\sum_{i=1}^{n} m_{i,i} - \sum_{i=1}^{n}(G_i C_i)}{N^2 - \sum_{i=1}^{n}(G_i C_i)} \quad (1)$$

where: i = class number; N = total number of classified values compared to truth values; $m_{i,i}$ = number of values belonging to the truth class i that have also been classified as class i; C_i = total number of predicted values belonging to class i; G_i = total number of truth values belonging to class i. Kappa values range from 0 to 1, with interpretation: κ < 0.40 (poor agreement), 0.40–0.59 (fair agreement), 0.60–0.79 (good agreement), 0.80–0.90 (perfect agreement), and > 0.90 (almost perfect agreement).

Carbon Stock Inventory and Quantification

Carbon stock calculation employed the IPCC Tier 1 approach using secondary emission factors with standardized international procedures enabling regional comparability with widely available data (Intergovernmental Panel on Climate Change, 2006). DW land cover classes were reclassified per the Technical Guidelines for Planning, Evaluation, and Reporting GHG Emission Reduction Actions (Bappenas, 2023). Carbon stock estimation was calculated by multiplying land cover area by secondary emission factors:

$$Carbon\ Stock = \sum_{i=1}^{n}(Area_{LC\,i}\ x\ Factor\ emission_{LC\,i}) \quad (2)$$

where: i = land cover type; $Area_{LC\,i}$ = area of land cover type i (hectares); $Factor\ emission_{LC\,i}$ = conversion factor for land cover type (tC/ha). Calculation was conducted spatially using zonal statistics functions in a GIS environment.

Accuracy testing of estimated values was then performed using the Relative Error method to assess the magnitude of deviation between estimated and actual values:

$$Relative\ error = \frac{Actual\ Value - Predicted\ Value}{Actual\ Value} \quad (3)$$

Smaller relative error values indicate that the carbon stock estimation increasingly approaches actual values, demonstrating greater model accuracy and reliability (Semito et al., 2025).

Carbon Stock Change and Temporal Dynamics Analysis

Carbon stock change analysis was conducted through spatial overlay technique between land cover maps of initial and final periods. Carbon Stock Change (ΔC) was calculated using:

$$\Delta C = C_{end} - C_{begin} \quad (4)$$

ΔC with negative values indicating emissions (carbon release) and positive values indicating sequestration (carbon uptake). Temporal trend analysis of carbon stock was performed using simple linear regression to determine carbon stock change tendency over time:

$$Y = a + bX \quad (5)$$

where: Y = carbon stock value (dependent variable); X = year (independent variable); a = intercept; b = slope or regression coefficient. Analysis was conducted using Microsoft Excel software through the Data Analysis – Regression feature. The b parameter (slope) represents the average annual change in carbon stock value. If b value is negative, there is a tendency for annual carbon stock decline, and if b is positive, there is an increasing tendency. The p-value for the Year parameter (slope) was analyzed to test statistical significance of the resulting trend. If p-value < 0.05, the trend is declared statistically significant.

Spatial Analysis of Carbon Release and Carbon Sequestration

Analysis was conducted using QGIS software through spatial intersection of carbon data between two different years, calculating change values using Field Calculator, and classification using Symbology features to display differences between carbon release and carbon sequestration areas. This analysis identifies critical regions and provides a basis for decision-making regarding carbon mitigation and restoration at the site level spatially.

Results and Discussion

Pre-Processing, Classification, and Validation of Temporal Land Cover Data

The systematic and standardized data pre-processing process as explained in the Methods ensures spatial-temporal consistency in the dataset for subsequent analysis. The integration of Google Earth Engine API and QGIS resulted in efficient processing of high-resolution data (10 m) without requiring high-capacity local hardware. DW classification for the 2016–2025 period demonstrate the spatial distribution of 9 land cover classes in Malang City (Figure 1). The spatial distribution exhibits characteristic urban patterns with Built (settlement/infrastructure) concentration in the city center and north, while Trees, Crops, and Shrub and Scrub are concentrated in southern, southeastern, and peri-urban areas. Water, Flooded Vegetation, and Grass are distributed in limited quantities. Bare and Snow/Ice areas are practically unidentified in the study area, consistent with Malang City's tropical climate location.

Analysis of DW data reveals LCC during the 2016–2025 (Table 1). The Built-up Land class consistently represents the largest land cover category, comprising approximately 77% of total area, demonstrating significant cumulative increase from 7,924.14 ha in 2016 to 8,869.86 ha in 2025, reflecting a 12% growth rate over nine years. Conversely, vegetative categories functioning as carbon storage show significant decline as follows:

- Trees (Forest Plantation) experienced sharp decrease from the highest peak of 2,126.79 ha (2017) to the lowest point of 1,162.71 ha (2023). Although a slight increase occurred on 2024-2025, the area decline from 2016 baseline to 2025 amounts to a total of 562.23 ha, highlighting massive land conversion to built-up areas.
- Crops (Dry Land Agriculture) shows declining trend from 1,031.04 ha (2016) to 753.12 ha (2025), experiencing a 277 ha decline, indicating that dry land agriculture has become a primary target for land conversion.

The data reveal sporadic and incidental land change patterns, meaning LCC occurs across many locations at different times. This underscores DW's advantage. DW data derived from Sentinel-2 with 10-meter spatial resolution and daily temporal resolution captures rapid and seasonal LCC frequently missed by conventional remote sensing data. Although individual changes are small and

Table 1. Land Cover Area

Land Cover Class	Year (Ha)									
	2016	2017	2018	2019	2020	2021	2022	2023	2024	2025
Water	32.85	8.64	1.80	1.08	4.05	5.04	7.56	1.62	7.47	14.31
Trees	1,980.00	2,126.79	1,603.80	1,465.65	1,776.51	1,849.77	1,696.41	1,162.71	1,171.26	1,417.77
Grass	46.26	28.80	14.67	7.74	26.55	32.94	27.90	9.99	16.92	32.31
Flooded Vegetation	86.85	53.10	4.41	5.94	31.50	26.37	15.57	1.62	8.46	14.94
Crops	1,031.04	873.72	1,146.69	1,135.80	835.92	713.25	769.68	972.18	922.95	753.12
Shrub And Scrub	4.59	3.78	13.86	7.29	1.98	2.97	0.27	9.36	5.04	1.80
Built	7,924.14	8,010.63	8,319.60	8,480.88	8,426.07	8,474.85	8,587.44	8,947.98	8,971.92	8,869.86
Bare	-	0.27	0.90	1.35	3.15	0.54	0.90	0.27	1.71	1.62

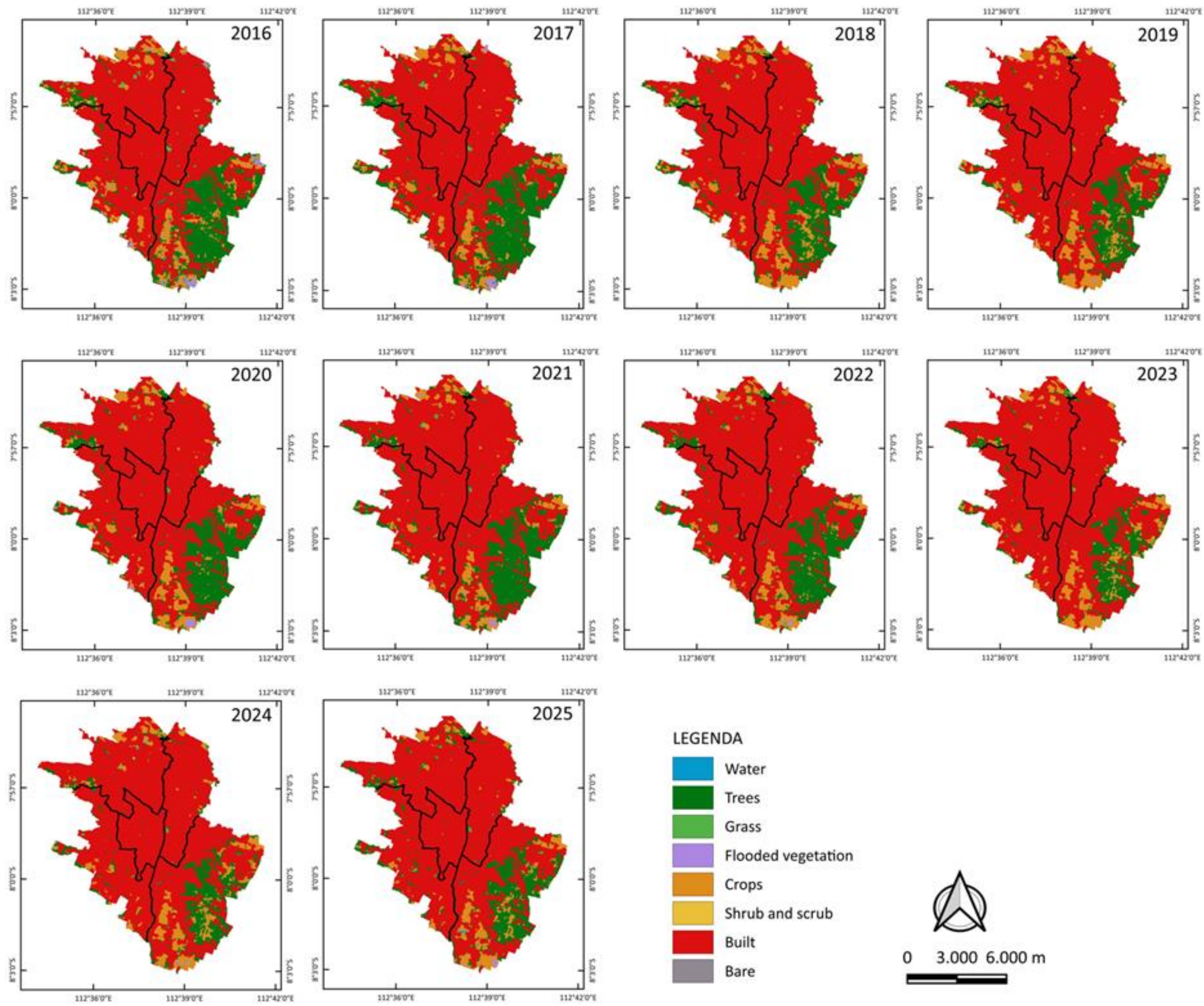

Fig. 1. Land cover change maps of Malang City from 2016 to 2025 based on Google Dynamic World data. Each panel displays the spatial distribution of main land cover categories for the respective year. Blue marks water bodies, dark green indicates trees, light green for grassland, purple for flooded vegetation, orange highlights cropland, yellow for shrub and scrub, red areas represent built-up land, and grey for bare soil. The dominant trend is the expansion of built-up areas (red) and decline in tree cover (green). Thick lines outline subdistrict administrative boundaries. Source: processed from Google Dynamic World (2016-2025)

dispersed, they collectively they contribute to substantial vegetation area reduction.

DW land cover classification validation results demonstrate Overall Accuracy (OA) of 94% and Kappa Coefficient of 0.91, indicating perfect classification accuracy suitable for further analysis. The high accuracy level (91%) is consistent with literature demonstrating DW achieves classification accuracy of 87–94% for various land contexts (Brown et al., 2022).

Carbon Stock Inventory and Quantification

DW land cover data with nine classes were reclassified into eight classes conforming to Technical Guidelines for Planning, Evaluation, and Reporting GHG

Emission Reduction Actions (Bappenas, 2023). The reclassification process and emission factor assignment are shown in Table 2.

Table 2. Reclassification Land Cover Class

DW Class	Technical Guidelines Class	Emission Factor
Water	Water	0
Trees	Forest Plantation	87.26
Grass	Grassland	4
Flooded Vegetation	Paddy Field	2
Crops	Dry Land Agriculture	10
Shrub And Scrub	Shrubland	30
Built	Settlement	4
Bare	Bare Land	2.5

Carbon stock calculation was performed using IPCC Tier 1 methodology based on land cover area multiplied by emission factors. Annual carbon stock calculation revealed total carbon stock reaching peak in 2017 (226,698.89 tC) and lowest point in 2023 (147,296.47 tC). The decline from 2016–2025 period totalled 48,335.78 tC (22.44%) with average carbon stock of 185,265.30 tC (16.68 tC/ha).

Carbon stock was classified into ranges Low (0–27,278.75 tC), Moderate (27,278.76–54,557.50 tC), High (54,557.51–81,836.25 tC), and Very High (81,836.26–109,116.00 tC), as demonstrated in Figure 2. The High and Very High classifications are concentrated in southern and southeastern Malang City areas, while Low and Moderate classifications dominate central and northern city regions. Fragmentation and diminution of the Very High zones are evident over time. This phenomenon is especially obvious in 2023–2025, primarily due to built-up expansion into southern and southeastern peri-urban areas.

Carbon stock spatial estimation accuracy testing using Relative Error metric shows values below 5%, indicating that DW and IPCC Tier 1 emission factor-based carbon stock estimation model achieves high accuracy and approaches actual values. The model can be determined accurate and reliable for subsequent temporal and spatial analysis.

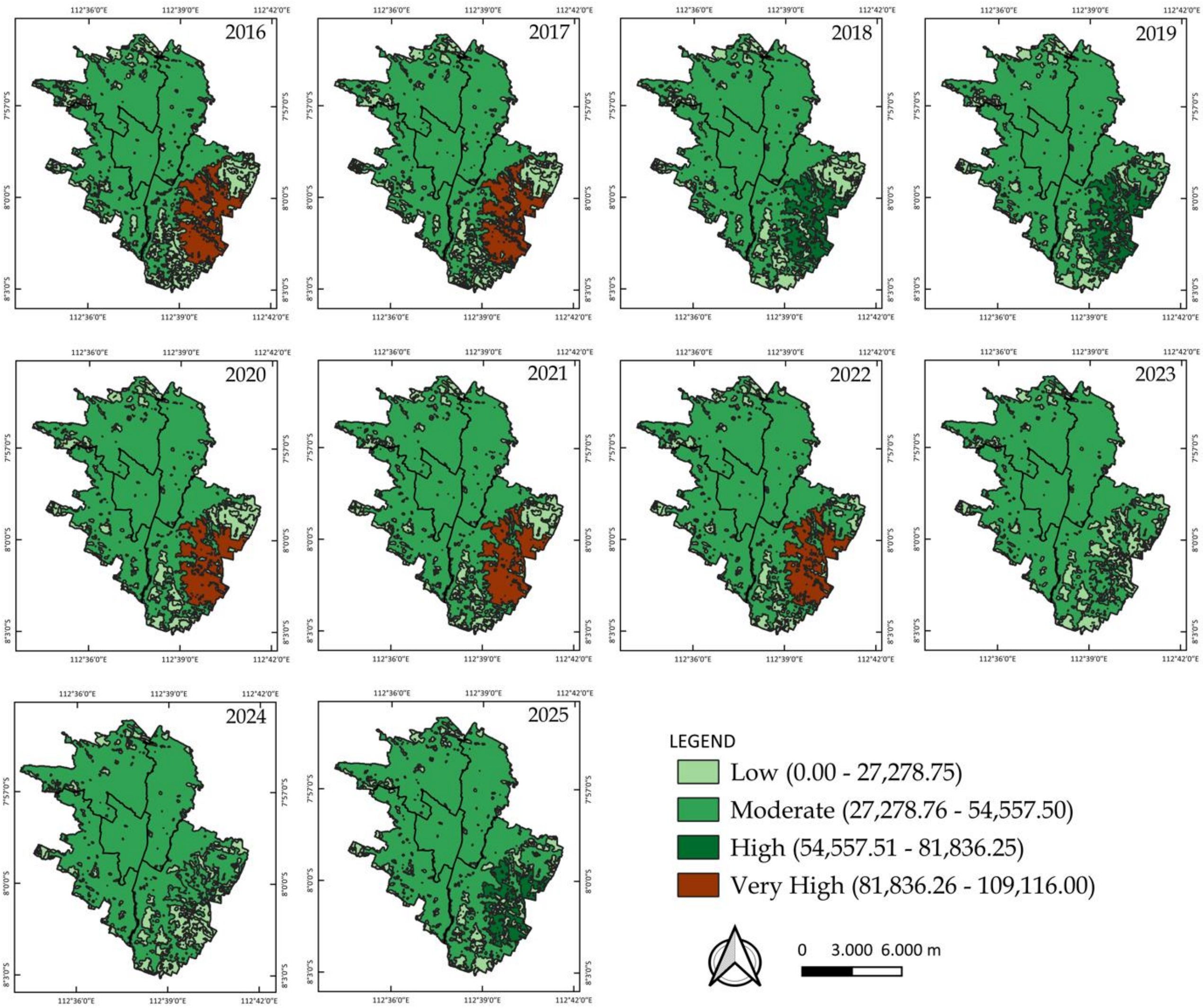

Fig. 2. Spatial distribution map of carbon stock in Malang City from 2016 to 2025. The map colors indicate carbon stock categories: very high (red), high (dark green), moderate (green), and low (light green). Carbon stock decline is observable from the shift in color from red to green throughout the analysis period. This trend is mainly driven by built-up expansion into the southern and southeastern peri-urban regions. Thick lines denote subdistrict boundaries. Source: processed from Google Dynamic World (2016-2025) and Bappenas 2023 emission factors

Table 3. Total Carbon Stock and Relative Error Validation Result

Year	Actual Carbon Stock (tC)	Predicted Carbon Stock (tC)	Average Carbon Stock per ha (tC/ha)	Relative Error
2016	215,278.20	215,260.20	19.38	0.01%
2017	226,698.89	226,653.89	20.40	0.02%
2018	185,178.44	185,142.44	16.67	0.02%
2019	173,439.05	173,358.05	15.61	0.05%
2020	197,318.22	197,282.22	17.76	0.02%
2021	202,717.78	202,699.78	18.25	0.01%
2022	190,228.39	190,201.39	17.13	0.01%
2023	147,296.47	147,287.47	13.26	0.01%
2024	147,561.90	147,525.40	13.28	0.02%
2025	166,942.42	166,798.42	15.03	0.09%

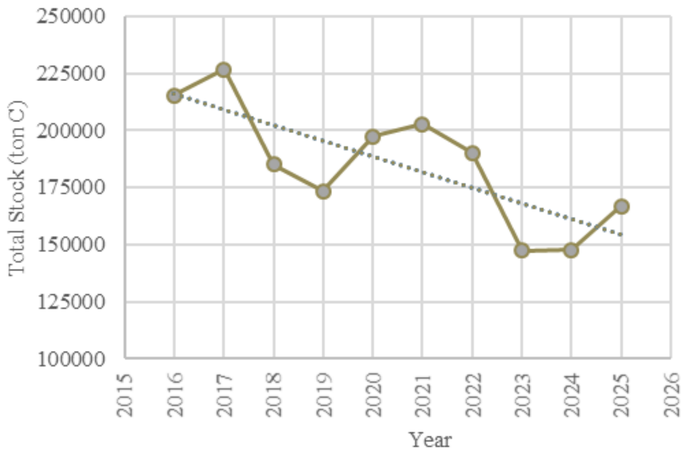

Fig. 1. Temporal Carbon Stock Change Trend

Average carbon stock estimate of 16.68 tC/ha for Malang City is classified as moderate for tropical urban contexts and consistent with several prior studies. Tropical cities with built-up land dominance typically retain only 5–10 tC/ha carbon (Murtala et al., 2019), while cities characterized by vegetation-urban area mixture can reach 15–25 tC/ha (Velasco & Chen, 2019). Studies of peri-urban and suburban areas with high residual vegetation coverage globally obtain values of 20–40 tC/ha as upper range (Arianasari & Kaskoyo, 2021).

Carbon stock calculation using IPCC Tier 1 Method excels through international standardization enabling comparability. However, Tier 1 limitation involves default emission factors potentially not reflecting local specifics (e.g., tree age, species type). Subsequent research with detailed field measurements (Tier 2/3) could enhance precision; however, for temporal monitoring and spatial hotspot identification purposes, Tier 1 proves sufficiently robust (Semito et al., 2025)

Carbon Stock Change and Temporal Dynamics Analysis

Carbon stock change analysis conducted by calculating final year carbon stock against 2016 baseline revealed total ΔC for 2016–2025 equals −48,335.78 tC (decline/emission). The negative ΔC value indicates that Malang City overall experienced carbon release during the observation period (Table 3).

Temporal trend analysis using simple linear regression with year (X) and carbon stock (Y) as variables revealed slope (b) of −6,803.80 tC/year, representing average annual decline (Figure 3). P-value of 0.009 (< 0.05) confirms that carbon stock decline trend is statistically significant and not a random occurrence. With 95% confidence level, Malang City can be said to undergo measurable consistent carbon stock decline, averaging 6,803.80 tC annually. The 22.44% decline over nine years represents substantial environmental degradation.

R^2 value of 0.594 means 59.4% of carbon stock variation can be explained by temporal change (year factor). The remainder (40.6%) is influenced by other factors such as specific land cover transition types (Fu et al., 2025), population growth, and economic structure (Luo et al., 2023). R^2 value of 0.594 still demonstrates reasonably strong relationship between time and carbon stock, validating linear regression use for trend characterization.

Malang City's carbon stock decline trend contrasts with national climate mitigation targets. Indonesia's NDC targeting increased carbon sink, however Malang City’s decline of 6,804 tC/year demonstrates Malang City has not yet contributed positively to national emission targets. Urgent intervention is needed to revitalize urban carbon sink.

Spatial Analysis of Carbon Release Zone

Figure 4 reveals that Malang City experienced predominant carbon release during most periods. Regions previously capable of carbon absorption have transformed into release areas, particularly in southern and southeastern areas. These historically vegetated buffer zones have transformed into annual carbon release hotspots due to environmental degradation. Nighttime light analysis confirms that outward urban sprawl into peri-urban zones drives vegetation-to-built conversion in these carbon-rich regions (Afrianto et al., 2025).

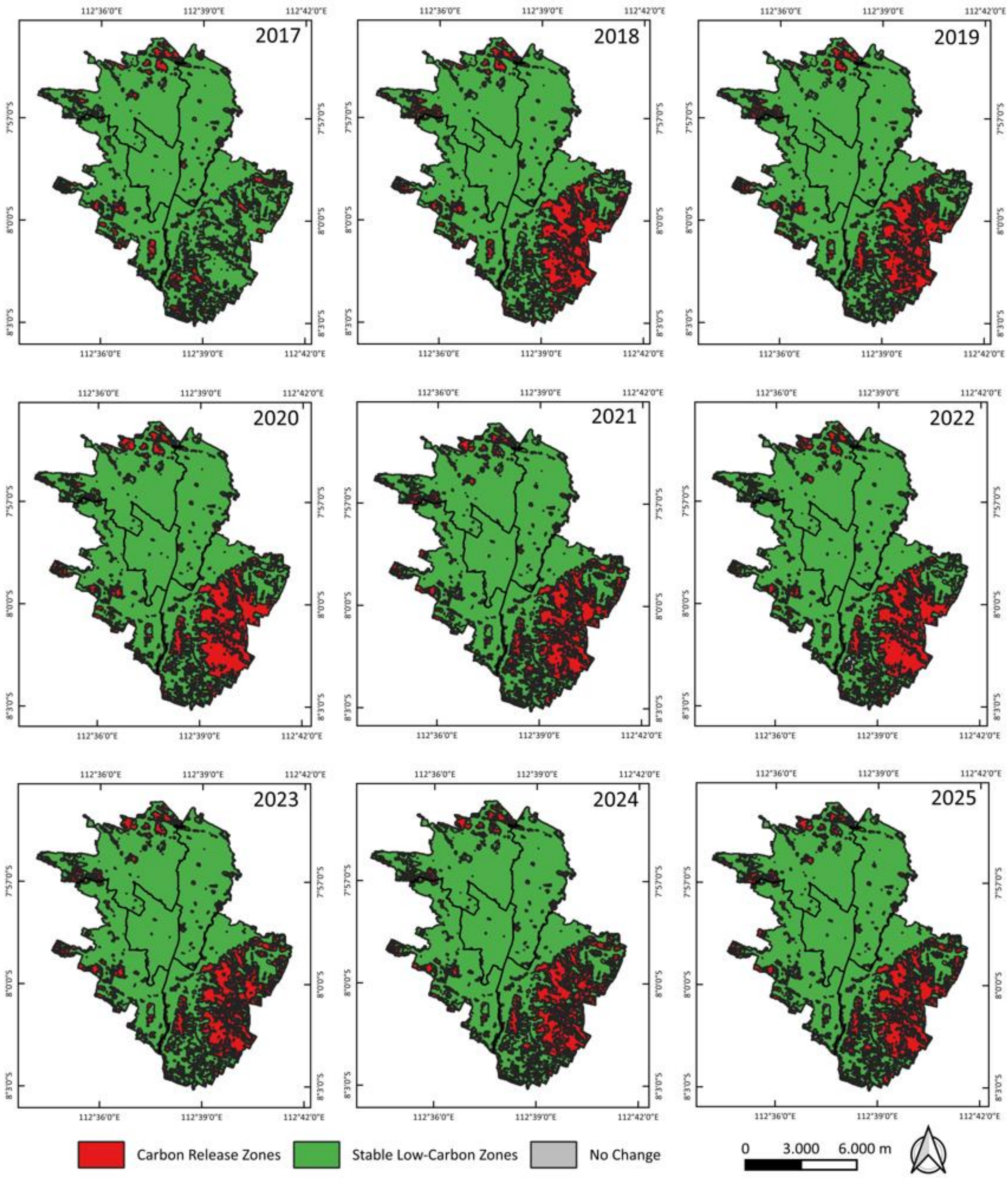

Fig. 4. Annual series maps of carbon release and stable areas in Malang City from 2017 to 2025. Red zones represent annual carbon release arising from intensive land cover change or conversion, particularly in the southern and southeastern. Green areas indicate regions with relatively stable land cover where carbon stock change remains low or negligible. Gray shows areas without carbon change. Black lines mark subdistrict administrative boundaries. Source: author's spatial analysis based on Google Dynamic World data (2016–2025)

Carbon Degradation Priority Zones shown in Figure 5 includes:

- Southern Malang City (dominant) - Trees/Crops conversion to Built occurs consistently during 2017-2025, indicating Entrenched Degradation due to residential and commercial development pressure.
- Southeast/Peri-Urban (significant) - Crops/Shrub conversion to Built occurs as area for horizontal development expands due to urban sprawl seeking cheaper land at periphery.

It should be noted that there are Stable Low-Carbon Zones with carbon uptake dominance occur in central and northern city regions. These areas have predominantly remained Built-up Land since 2016 baseline without LCC through 2025. As a result, these zones maintain relatively stable and low carbon stock values, rather than exhibiting active carbon uptake.

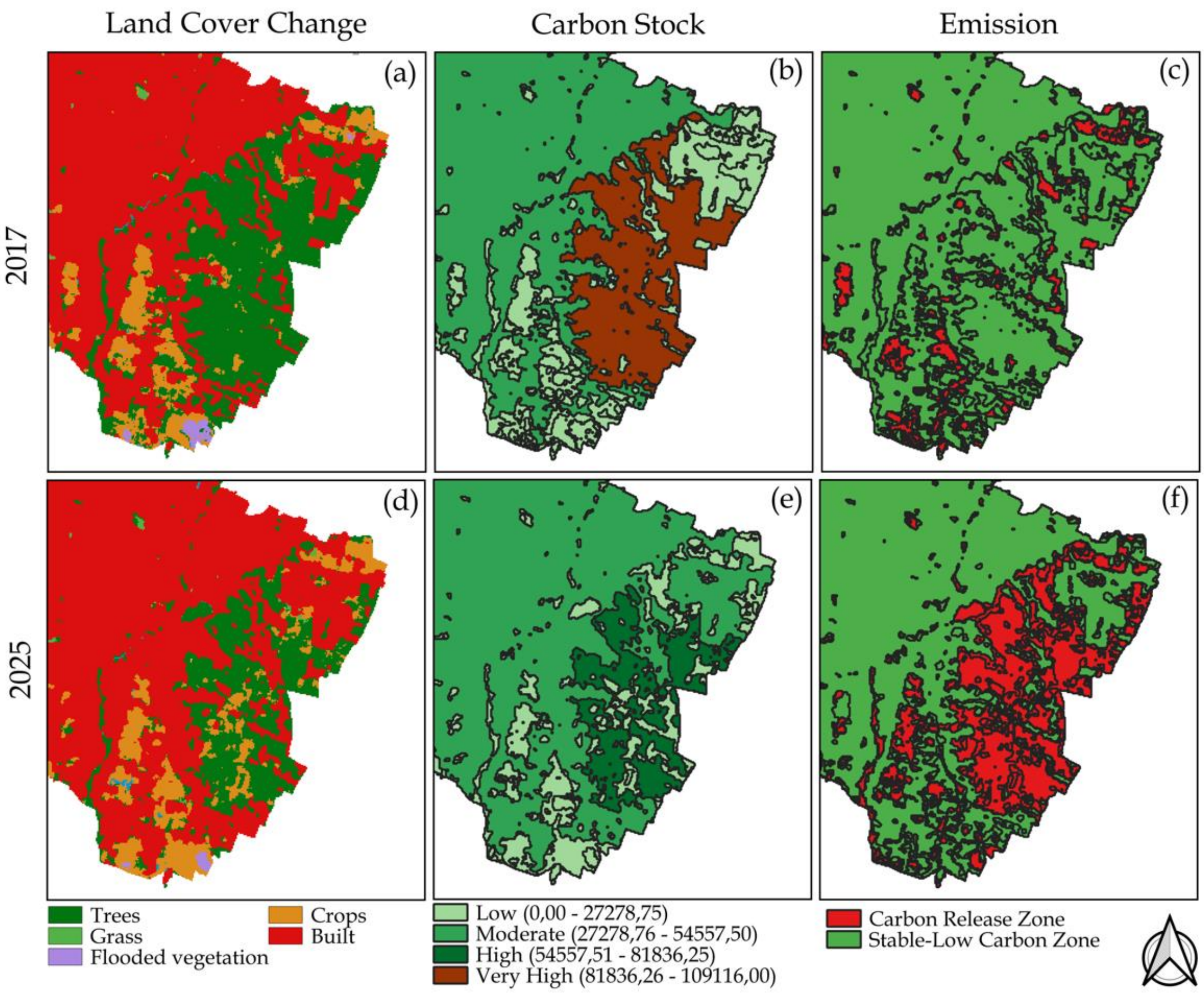

Fig. 5. Carbon Degradation Priority Zones (southern and southeastern city areas): (a) Land cover 2017; (b) Spatial carbon stock classification 2017; (c) Spatial change classification (release and stable-low) 2017; (d) Land cover 2025; (e) Spatial carbon stock classification 2025; (f) Spatial change classification. The figure demonstrates that, between 2017 and 2025, land cover transitions to built-up areas have occurred. This conversion has led to a decline in carbon stock levels from very high to high, indicating significant carbon release in these areas

In summary of the results, the specific action plans applicable to Malang City conditions include:

1. Land Use Control through Spatial Planning regulation (Lwasa et al., 2023) to classify Carbon Release Hotspots as priority conservation zones.
2. Strict Zoning Regulations to prevent horizontal building expansion into vegetation areas (Transport for NSW, 2022).
3. High-Rise Buildings to promote vertical development in already saturated central city land areas (Soares et al., 2025).
4. Building Decarbonization to implement green building requiring low-carbon materials and energy-efficient design (Soares et al., 2025).
5. Urban Forest and Green Corridors to prioritize carbon sequestration capacity enhancement through development (John-Rob Pool (WRI) et al., 2023). Recent study show green corridors of Malang City contributed 1.69% toward regional mitigation targets (Nandini et al., 2024).
6. Green Roofs, Green Walls, Urban Farms, developing green infrastructure on Carbon Sequestration Hotspot buildings (ICOS, 2025), and integrating trees and food plants (Costa Jr et al., 2023) with vertical farming to avoid increased land footprint (H. Liu et al., 2025).
7. Payment for Ecosystem Services, providing incentive-based compensation ensuring peri-urban landowners with stable tree or crop coverage to resist land-conversion pressures (Liu et al., 2025). It effectively offers financial compensation for maintaining carbon storage land function, such as agroforestry.

Environmental contamination and degradation occur systematically across various sectors (Anggayasti et al., 2024), emphasizing integrated spatial planning approach necessity responsive to climate change issues. These interventions ensure spatial planning policy not only reacts to already-occurred degradation but proactively protects remaining and potential carbon stock, enhancing Malang City's climate resilience consistent with local-level climate change mitigation objectives.

Conclusion

This research has identified and quantified Malang City carbon stock dynamics during 2016–2025, revealing a statistically significant decline of 48,335.78 tC (−22.44%) with an annual average loss of 6,803.80 tC ($p = 0.009$). This decline reflects substantial environmental degradation in Malang City's carbon storage capacity. Spatial analysis highlights Carbon Release Hotspots, areas where vegetated covers (such as trees, crops, and shrub) was converted to built-up land. Conversely, Stable Low-Carbon Zones in central and northern regions are characterized by built-up land with consistently low and stable carbon stock values without active sequestration.

By distinguishing between carbon stock (total stored carbon) and carbon sequestration (annual uptake by growing vegetation), this study offers a solid foundation for spatially targeted mitigation and adaptation. These findings demonstrate the utility of high-resolution remote sensing for spatially explicit urban carbon monitoring and climate-responsive planning in tropical environments.

Limitations

This study has two main limitations. First, ground truth validation was only performed for 2025 due to lack of historical field data, introducing uncertainty in baseline carbon stock estimates. Second, the average sample size per land cover class (≈11 points) is below recommended remote sensing standards, which may affect robustness of accuracy metrics. Future research should expand validation to earlier years and employ more samples per class to improve reliability and generalizability of mapping results.

Acknowledgement

The authors would like to thank The Ministry of National Development Planning and the Malang City Government for financial support.

References

Afrianto, F., Hariyanto, A. D., & Tucunan, K. P. (2025). Nighttime Lights as Indicators of Energy Efficiency Across Urban Morphologies in Malang City. *Journal of Regional and City Planning*, *36*(1), 68–91. https://doi.org/10.5614/jpwk.2025.36.1.5

Anggayasti, W. L., Sudaryanti, S., Pertiwi, M., Nurjannah, R. S. F., Sheviyandini, T. Y., Suryatama, J., Rubiyatadji, R., Koentjoro, M. P., & Kurniawan, A. (2024). Identifying the distribution and source of riverine plastic waste contamination: case study of Brantas River in Malang city. *Eastern-European Journal of Enterprise Technologies*, *5*(10 (131)), 37–44. https://doi.org/10.15587/1729-4061.2024.313830

Arianasari, V., & Kaskoyo, H. (2021). Estimasi Simpanan Karbon di Atas Permukaan Tanah pada Hutan Rakyat di Kawasan Perkotaan, Kota Bandar Lampung, Provinsi Lampung. *Jurnal Ilmu Kehutanan*, *15*(2), 174–184. https://doi.org/10.22146/jik.v15i2.1537

Bappenas. (2023). *Petunjuk Teknis Perencanaan, Evaluasi dan Pelaporan Aksi PRK*.

Brown, C. F., Brumby, S. P., Guzder-Williams, B., Birch, T., Hyde, S. B., Mazzariello, J., Czerwinski, W., Pasquarella, V. J., Haertel, R., Ilyushchenko, S., Schwehr, K., Weisse, M., Stolle, F., Hanson, C., Guinan, O., Moore, R., & Tait, A. M. (2022). Dynamic World, Near real-time global 10 m land use land cover mapping. *Scientific Data*, *9*(1), 251. https://doi.org/10.1038/s41597-022-01307-4

Cahyono, W. E., Parikesit, Joy, B., Setyawati, W., & Mahdi, R. (2022). Projection of CO2 emissions in Indonesia. *Materials Today: Proceedings*, *63*. https://doi.org/10.1016/j.matpr.2022.04.091

Costa Jr, C., Thornton, P., & Wollenberg, E. (2023). Global hotspots of climate change adaptation and mitigation in agriculture. *Frontiers in Sustainable Food Systems*, *7*. https://doi.org/10.3389/fsufs.2023.1216205

Fu, S., Peng, Y., Xu, B., Feng, Y., Yu, J., Zeng, X., & Zhang, X. (2025). Investigating the effects of urban expansion on carbon stocks and developing optimization strategies: A case study of Nanchang. *Ecological Frontiers*, *45*(5), 1486–1497. https://doi.org/10.1016/j.ecofro.2025.06.017

ICOS (Integrated Carbon Observation System). (2025). Cities: from emission hotspots to climate action innovators. *Fluxes Magazine, Volume 4*. https://www.icos-cp.eu/sites/default/files/2025-10/Fluxes_Vol4_2025_Single_page.pdf

Intergovernmental Panel on Climate Change. (2006). IPCC Guidelines for National Greenhouse Gas Inventories. *Agriculture, Forestry and Other Land Use*, *4*.

IPCC. (2019). *Report on Climate Change and Land*. https://www.ipcc.ch/srccl/

Isdianto, A., Hasyim, A. W., Sukojo, B. M., Alimuddin, I., Anggraini, I. A., & Fatahillah, E. R. (2025). Integrating Urban Design with Natural Dynamics: Enhancing Ecological Resilience in Malang City over a Decade. *International Journal of Sustainable Development and Planning*, *20*(3), 1061–1075. https://doi.org/10.18280/ijsdp.200313

John-Rob Pool (WRI), David Gibbs (WRI), Sadof Alexander (WRI), & Nancy Harris (WRI). (2023). *5 Reasons Cities Should Include Trees in Climate Action*. https://wri-indonesia.org/en/insights/5-reasons-cities-should-include-trees-climate-action-0

Liu, H., Zhang, J., & Wang, Z. (2025). Assessing and optimizing the potential for climate change mitigation and carbon sequestration in urban residential green spaces: energizing sustainable cities. *Frontiers in Environmental Science*, *13*. https://doi.org/10.3389/fenvs.2025.1519297

Liu, Y., Mei, X., Yue, L., & Zhang, M. (2025). Response of carbon storage to land use change and multi-scenario predictions in Zunyi, China. *Scientific Reports*, *15*(1), 236. https://doi.org/10.1038/s41598-024-81444-5

Luo, M., Liu, H., Gao, J., Tang, Y., Guo, L., Pi, J., & Yu, Y. (2023). Spatiotemporal Variations and Influencing Factors of Urban Carbon Sink: A Case Study of Wuhan, China. *Ecosystem Health and Sustainability*, *9*. https://doi.org/10.34133/ehs.0133

Lwasa, S., Seto, K. C., Bai, X., Blanco, H., Gurney, K. R., Kilkis, S., Lucon, O., Murakami, J., Pan, J., Sharifi, A., & Yamagata, Y. (2023). Urban Systems and Other Settlements. In *Climate Change 2022 - Mitigation of Climate Change* (pp. 861–952). Cambridge University Press. https://doi.org/10.1017/9781009157926.010

Murtala, D., Abd Manaf, L., Ramli, M. F., Yacob, M. R., & A. Makmom, A. (2019). Quantifying The Aboveground Biomass And Carbon Storage Of Urban Tree Species In Sokoto Metropolis, North-Western Nigeria. *PLANNING MALAYSIA*, *17*. https://doi.org/10.21837/pm.v17i10.639

Nandini, S., Kartikaningsih, H., Semedi, B., & Koentjoro, M. P. (2024). Carbon sequestration potential of green corridor to reduce transportation greenhouse gas emissions: a case study in Malang City. *Berkala Penelitian Hayati*, *30*(3), 130–136. https://doi.org/10.23869/bphjbr.30.3.20245

NV5 Geospatial Solutions, I. (2024). *Calculate Confusion Matrices*. https://www.nv5geospatialsoftware.com/docs/CalculatingConfusionMatrices.html

Pambudi, P. A., Anggraeni, P. D., & Handoko, R. S. (2024). *Pambudi+et+al.+(2024)*. *1*(1), 4–20.

Rahman, F. A., Mubarokah, N., Yuhardi, E., Adiputra, A., Supriyadi, S., & Suryawati, S. (2023). Perubahan Tutupan Lahan dan Stok Karbon Permukaan di Daerah Aliran Sungai (DAS) Blega. *Jurnal Sumberdaya Alam Dan Lingkungan*, *10*(2), 69–78. https://doi.org/10.21776/ub.jsal.2023.010.02.3

Semedi, B., Samsu Rijal, S., Sambah, A., & Isdianto, A. (2021). *Pengantar Pengindraan Jauh Kelautan*.

Semito, M. A. P. N., Soenardjo, N., & Pramesti, R. (2025). Pendugaan Stok Karbon Mangrove Menggunakan Citra Sentinel-2A Di Segara Anakan, Cilacap. *Journal of Marine Research*, *14*(3), 517–527. https://doi.org/10.14710/jmr.v14i3.47702

Soares, F., Silva, M. C., & Azevedo, I. (2025). Urban decarbonization policies and strategies: A sectoral review. *Renewable and Sustainable Energy Reviews*, *215*, 115617. https://doi.org/10.1016/j.rser.2025.115617

Tavasoli, N., Arefi, H., & Esfahany, S. S. (2019). *Modelling The Amount Of Carbon Stock Using Remote Sensing*. *October*. https://doi.org/10.5194/isprs-archives-XLII-4-W18-1051-2019

Transport for NSW (New South Wales Government). (2022). *Net Zero Cities Action Plan*. Government Strategy Document. https://www.transport.nsw.gov.au/industry/cities-and-active-transport/net-zero-cities-action-plan

Velasco, E., & Chen, K. W. (2019). Carbon storage estimation of tropical urban trees by an improved allometric model for aboveground biomass based on terrestrial laser scanning. *Urban Forestry & Urban Greening*, *44*, 126387. https://doi.org/10.1016/j.ufug.2019.126387

Venter, Z. S., Barton, D. N., Chakraborty, T., Simensen, T., & Singh, G. (2022). Global 10 m Land Use Land Cover Datasets: A Comparison of Dynamic World, World Cover and Esri Land Cover. *Remote Sensing*, *14*(16), 4101. https://doi.org/10.3390/rs14164101